AD-A086 138 BATTELLE COLUMBUS LABS OH F/G 5/8
DETECTABILITY OF OBJECTS IN SPECKLE.(U)
OCT 79 A KOZMA DAAG29-76-D-0100
UNCLASSIFIED DRSMI/RR-CR-80-1 NL

1 OF 1
AD
A086138

END
DATE
FILMED
8-80
DTIC

LEVEL II

(12)

ADA086138

TECHNICAL REPORT RR-CR-80-1

DETECTABILITY OF OBJECTS IN SPECKLE

Adam Kozma
Environmental Research Institute of Michigan
Ann Arbor, Michigan

Prepared for:

Research Directorate
US Army Missile Laboratory

October 1979

U.S. ARMY MISSILE COMMAND
Redstone Arsenal, Alabama 35809

DDC FILE COPY

Approved for public release; distribution unlimited.

SMI FORM 1021, 1 JUL 79 PREVIOUS EDITION IS OBSOLETE

DISPOSITION INSTRUCTIONS

DESTROY THIS REPORT WHEN IT IS NO LONGER NEEDED. DO NOT RETURN IT TO THE ORIGINATOR.

DISCLAIMER

THE FINDINGS IN THIS REPORT ARE NOT TO BE CONSTRUED AS AN OFFICIAL DEPARTMENT OF THE ARMY POSITION UNLESS SO DESIGNATED BY OTHER AUTHORIZED DOCUMENTS.

TRADE NAMES

USE OF TRADE NAMES OR MANUFACTURERS IN THIS REPORT DOES NOT CONSTITUTE AN OFFICIAL ENDORSEMENT OR APPROVAL OF THE USE OF SUCH COMMERCIAL HARDWARE OR SOFTWARE.

UNCLASSIFIED

SECURITY CLASSIFICATION OF THIS PAGE (When Data Entered)

REPORT DOCUMENTATION PAGE

READ INSTRUCTIONS BEFORE COMPLETING FORM

1. REPORT NUMBER RR-CR-80-1	2. GOVT ACCESSION NO. AD-A086138	3. RECIPIENT'S CATALOG NUMBER
4. TITLE (and Subtitle) DETECTABILITY OF OBJECTS IN SPECKLE		5. TYPE OF REPORT & PERIOD COVERED Technical Report
		6. PERFORMING ORG. REPORT NUMBER
7. AUTHOR(s) Adam Kozma		8. CONTRACT OR GRANT NUMBER(s)
9. PERFORMING ORGANIZATION NAME AND ADDRESS Environmental Research Institute of Michigan P.O. Box 8618 Ann Arbor, Michigan 48107		10. PROGRAM ELEMENT, PROJECT, TASK AREA & WORK UNIT NUMBERS
11. CONTROLLING OFFICE NAME AND ADDRESS Commander US Army Missile Command ATTN: DRSMI-RPT Redstone Arsenal, Alabama 35809		12. REPORT DATE October 1979 13. NUMBER OF PAGES 24
14. MONITORING AGENCY NAME & ADDRESS (if different from Controlling Office) Commander US Army Missile Command ATTN: DRSMI-RR Redstone Arsenal, Alabama 35809		15. SECURITY CLASS. (of this report) Unclassified 15a. DECLASSIFICATION/DOWNGRADING SCHEDULE

16. DISTRIBUTION STATEMENT (of this Report)

Approved for public release; distribution unlimited.

17. DISTRIBUTION STATEMENT (of the abstract entered in Block 20, if different from Report)

18. SUPPLEMENTARY NOTES

19. KEY WORDS (Continue on reverse side if necessary and identify by block number)

Speckle, Detection, Coherent images

20. ABSTRACT (Continue on reverse side if necessary and identify by block number)

Theoretical work based on the statistical techniques of hypothesis testing applied to speckle noise in coherent images is extended. It is shown that this theory can be applied to determination of probabilities of detection for low and medium contrast objects immersed in speckle noise.

DD FORM 1 JAN 73 1473 EDITION OF 1 NOV 65 IS OBSOLETE

UNCLASSIFIED

SECURITY CLASSIFICATION OF THIS PAGE (When Data Entered)

CONTENTS

I. INTRODUCTION

When diffuse objects are illuminated with coherent radiation, the appearance of the image is degraded by the presence of speckle. The effect of the speckle is to superimpose a noise-like structure which masks the spatial information present in the image.

Considerable work has been done in characterizing the speckle over the last few years [1]. Both theoretical and experimental work has revealed new ideas which have enhanced our understanding of the speckle phenomena.

The purpose of this work is to extend the statistical techniques of hypothesis testing first used by Dainty [2] to study speckle and to apply these extended techniques to the data generated in the studies conducted by Guenther et al. [3,4].

Dainty used simple statistical detection theory to study the problem of detecting small images immersed in a background of laser-produced speckle. He assumed that the detection device was a flying-spot scanner and showed that the size and transmittance of the scanning aperture was best determined by statistical considerations and not by signal-to-noise (SNR) criteria. He also showed that the typical detection problem of locating opaque disks in a speckle background requires that the geometrical image diameter be at least four times the Rayleigh resolution limit of the lens used to form the image for reliable detection. The work by Dainty was theoretical; no experimental data were presented to test his theory.

On the other hand, the work in References 3 and 4 was largely experimental with estimates of detection determined empirically. In that work, a special test target patterned after one first used by Rose is used. The target has disks of varying transmissivity and diameter which are imaged in the presence of speckle. The transmittance of the disks varies from 0.88 to 0.012, while the size varies from about two times the speckle size to about 14 times the speckle size. The test target is imaged under various illumination conditions.

In the following we will present, in a clear way, the theory first proposed by Dainty and show how this theory can apply to the experimental work of Guenther et al.

II. TESTING OF SIMPLE HYPOTHESIS [5]

In hypothesis testing, an observer measures a single quantity X and on the basis of this measurement chooses between two hypotheses H_0 or H_1. If X always was equal to a_0 when the hypothesis H_0 was true and to a_1 when H_1 was true, there would be no need for statistical hypothesis testing. However, because we may make errors in measurement or we have factors operating which we do not understand, the observation quantity X is a random variable that we can describe statistically by giving a probability density function $p_0(X)$ or $p_1(X)$ if H_0 or H_1 applies. The hypotheses are called simple if both $p_0(X)$ and $p_1(X)$ are completely known and they do not depend on unknown parameters.

A strategy must be adopted by the observer which assigns one hypothesis or the other to each observable outcome. This strategy divides the possible values of X into two ranges, R_0 and R_1, so that if X lies in R_0, H_0 is chosen and if X lies in R_1, H_1 is chosen. The regions should be so determined as to get the best average results in the experiment.

A simple example of this statistical test is to choose between two hypotheses:

H_0: rain tomorrow

H_1: no rain tomorrow

A possible way of obtaining such a decision is to determine the average rate of change of barometric pressure during the past 24 hours.

Suppose that

$p_0(X)$ is the p.d.f. of rates X on days before rain =

$$\left(2\pi\sigma^2\right)^{-\frac{1}{2}} \exp\left[-(X - a_0)^2/2\sigma^2\right]$$

$p_1(X)$ is the p.d.f. of rates X on days before no rain =

$$\left(2\pi\sigma^2\right)^{-\frac{1}{2}} \exp\left[-(X - a_1)^2/2\sigma^2\right]$$

where $a_0 < 0 < a_1$.

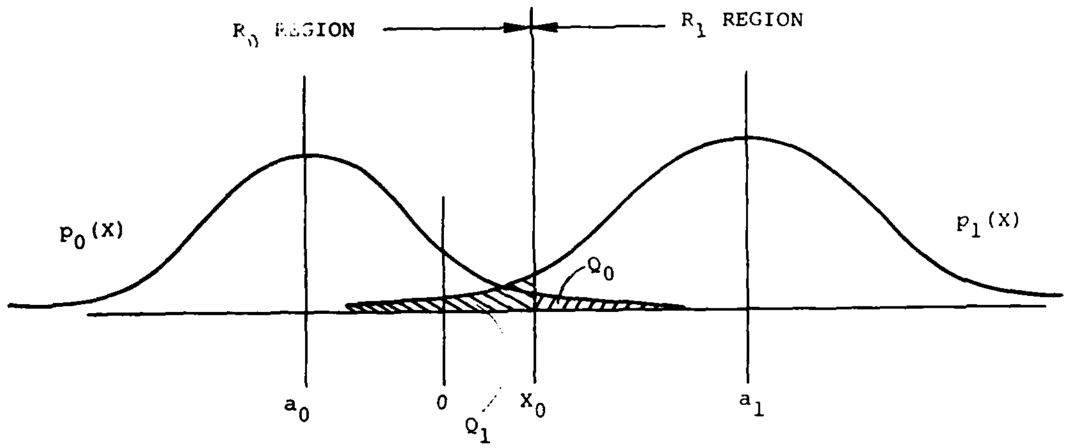

Figure 1. Probability density functions under hypotheses H_0 and H_1.

These p.d.f.'s are shown in Figure 1. We can see that on days before rain the barometer fell with an average rate a_0 which is negative, while on days before no rain the average rate is positive because the barometer was rising. In addition to the above data contained in the p.d.f., suppose we know the fraction ζ of rainy days that occurred in the past. This number ζ can be called the prior probability of rain and $(1 - \zeta)$ the prior probability of no rain.

As we can see in Figure 1, the p.d.f.'s overlap; thus, no matter how we choose regions R_0 and R_1, we will occasionally make a wrong decision. In fact, the probability of choosing H_1 when H_0 is true, so-called error of the first kind, is

$$Q_0 = \int_{X_0}^{\infty} p_0(X)\, dx,$$

shown as the crosshatched area under the $p_0(X)$ curve. The probability of choosing H_0 when H_1 is true, an error of the second kind, is

$$Q_1 = \int_{-\infty}^{X_0} p_1(X)\, dx.$$

The value of X_0 which the observer will choose depends on how much wrong decisions cost. Support that C_0 is the cost of an error of the first kind, C_1 is the cost of an error of the second kind, and C_0Q_0 and C_1Q_1 are called the risk associated with H_0 and H_1, respectively. Then the average risk of each decision is

$$\bar{C}(X_0) = \zeta C_0 Q_0 + (1 - \zeta)\, C_1 Q_1$$

$$= \zeta C_0 \int_{X_0}^{\infty} p_0(X)\, dx + (1 - \zeta)\, C_1 \int_{-\infty}^{X_0} p_1(X)\, dx.$$

We can minimize the above by differentiating with respect to X_0 and putting the result equal to zero. Thus,

$$\frac{p_1(X_0)}{p_0(X_0)} = \frac{\zeta C_0}{(1 - \zeta) C_1} = \Lambda_0$$

which yields

$$X_0 = (a_0 + a_1)/2 + \frac{\sigma^2}{a_1 - a_0} \ln \frac{\zeta C_0}{(1 - \zeta) C_1} .$$

Note that if $\zeta = 1/2$ and $C_0 = C_1$, we get $X_0 = (a_0 + a_1)/2$.

III. BAYES CRITERION

The Bayes criterion is a rule which allows the decision strategy to be picked so as to minimize the average risk.

There are four types of costs possible which can be arrayed in a cost matrix C.

$$C = \begin{bmatrix} C_{00} & C_{01} \\ C_{10} & C_{11} \end{bmatrix}$$

where C_{ij} is the cost of choosing H_i when H_j is true (i, j = 0, 1). The relative cost of error of the first kind is $C_{10} - C_{00}$ and of the second kind $C_{01} - C_{11}$, with both relative costs being positive. In the example,

$$C = \begin{bmatrix} 0 & C_1 \\ C_0 & 0 \end{bmatrix} .$$

In the general case where elements of the cost matrix are not zero, we have the average per decision as

$$\bar{C} = \zeta \left[C_{00} \int_{-\infty}^{X_0} p_0(X)\ dx + C_{10} \int_{X_0}^{\infty} p_0(X)\ dx \right]$$
$$+ (1 - \zeta) \left[C_{01} \int_{-\infty}^{X_0} p_1(X)\ dx + C_{11} \int_{X_0}^{\infty} p_1(X)\ dx \right] .$$

It can be shown that the average risk is minimum when X_0 is chosen so that, given the likelihood ratio

$$\Lambda(X) = p_1(X)/p_0(X) ,$$

R_0 consists of values of X for which $\Lambda(X) < \Lambda_0$ and R_1 consists of values of X for which $\Lambda(X) > \Lambda_0$ where Λ_0 is

$$\Lambda_0 = \frac{\zeta(C_{10} - C_{00})}{(1 - \zeta)(C_{01} - C_{11})} .$$

If ζ, the prior probability is known and values can be assigned to C_{ij} and the threshold X_0 dividing regions R_0 and R_1 can be found which minimizes the average risk for each decision. For the general cost of the detection of signals in noise, it is often the case that we cannot reasonably assign risks nor can we know prior probabilities; the position of the threshold is set from experiment by trial and error.

IV. SIGNALS IN NOISE

The theory outlined above is often used in the design of communications and radar systems. There, often the problem is to determine whether a signal and additive noise are being observed or whether noise alone is present.

In this case, the situation is illustrated in Figure 2. Here the crosshatched area A_1 under the p.d.f. curve of signal + noise gives the probability of detection while the doubly crosshatched area A_2 under the p.d.f. curve of noise alone is the probability of a false alarm. The problem here is determining the proper signal-to-noise ratio and threshold to give an adequate probability of detection while keeping the probability of a false alarm properly low. The SNR, which determines the relative position of the p.d.f. of signal + noise to the p.d.f. of noise alone, along with the proper choice of threshold, allows obtaining proper values of detection and false alarms.

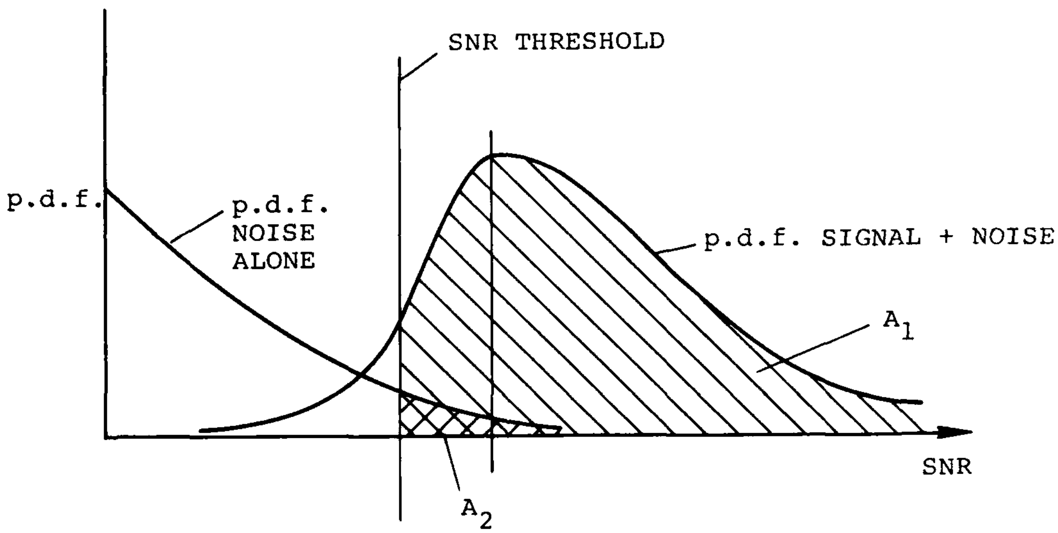

A_1=probability of detection A_2=probability of false alarm

Figure 2. Probability of noise alone and signal + noise illustrating the process of threshold detection.

V. DISK IMAGES IN SPECKLE

Suppose we have disk objects of intensity transmissivity $\langle T_i \rangle$ backed by a ground glass with average transmissivity of $\langle T_S \rangle$ where we assume $\langle T_S \rangle > \langle T_i \rangle$. The diameter of the disk is given by d where $d \geq d_S$. The quantity

d_S is the approximate size of the speckle as determined by the Rayleigh criterion. That is, $d_S = \frac{\lambda F}{D}$, where F is the focal length of the lens and λ is the wavelength of the light. Figure 3 illustrates this situation.

Suppose further that we place a photocell at plane P_3 with a diameter of d_p. This photocell is used to measure the amount of light which is present at this plane. We can use the voltage reading from the photocell to determine if a disk is present or not. The intensity measured by the photocell is

$$I_p = \iint_{-\infty}^{\infty} I(x,y)\ B(x,y)\ dxdy \qquad (1)$$

where $I(x,y)$ is the intensity distribution at P_3 and

$$\begin{aligned} B(x,y) &= 1 \text{ for } x^2 + y^2 \leq d_p \\ &= 0 \text{ otherwise;} \end{aligned} \qquad (2)$$

$I(x,y)$ can either be the intensity due to the presence of a disk in which case its average value as a function of x and y is given by

$$\langle I(x,y)\rangle_d = |0_A(x,y)|^2 * |K(x,y)|^2 \qquad (3)$$

where

$$\begin{aligned} |0_A(x,y)|^2 &= I \langle T_i\rangle \langle T_S\rangle \text{ for } x^2 + y^2 \leq d^2 \\ &= I\langle T_S\rangle \text{ otherwise;} \end{aligned} \qquad (4)$$

I is the uniform intensity of the laser illumination and $|K(x,y)|^2$ is the intensity point spread function of the optical system given by

$$|K(x,y)|^2 = \left(\frac{kD^2}{8F}\right)^2 \left[2\, \frac{J_1\left(\frac{kDr_0}{2F}\right)}{\frac{kDr_0}{2F}}\right] \qquad (5)$$

where $k = 2\pi/\lambda$, $J_1(X)$ is the first-order Bessel function and $r_0^2 = x^2 + y^2$. $I(x,y)$ will vary around $\langle I(x,y)\rangle$ due to the presence of speckle superimposed over the disk image by the ground glass.

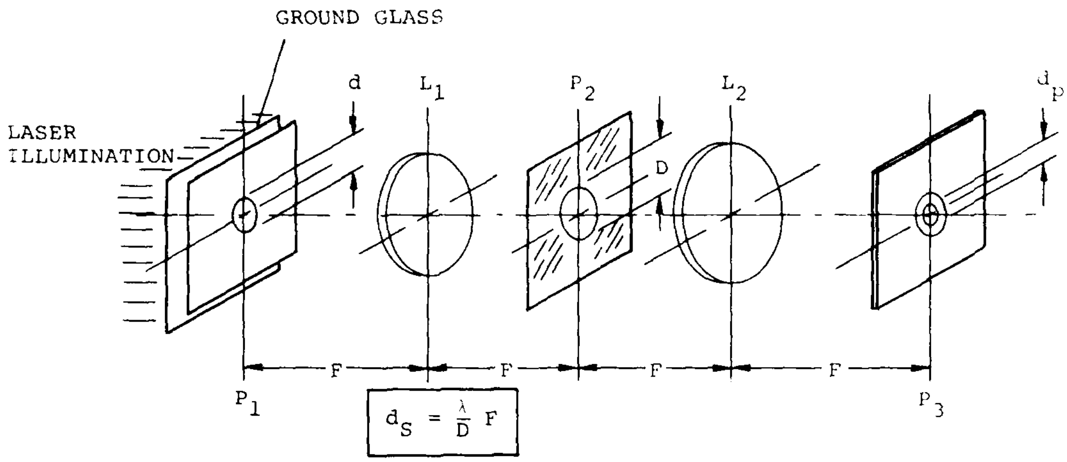

Figure 3. Imaging a dark disk with a coherent optical system in the presence of speckle noise.

If there is no disk present in plane P_1, then the intensity $I(x,y)$ is the intensity of the imaged ground glass. The average value of this intensity is given by

$$\langle I(x,y)\rangle_{nd} = I\langle T_S\rangle . \tag{6}$$

Again, $I(x,y)$ will vary around the average $\langle I\rangle$ because of the ground glass.

The p.d.f. associated with the photocell reading due to the intensity variation when no disk is present is given by $p_0(I)$, while the p.d.f. associated with the photocell reading when a disk is present is given by $p_1(I)$. The p.d.f.'s are shown in Figure 4. Generally, the p.d.f.'s will overlap and with a threshold I_T sometimes the wrong decision will be made whether a disk is or is not present. Two kinds of errors can be made. Errors of the first kind are the apparent detection of an image when it is not present. This false alarm probably α is given by

$$\alpha = \int_0^{I_T} p_0(I)\, dI \tag{7}$$

and is shown as the filled in area under the $p_0(I)$ curve in Figure 4. The second kind of error is in not detecting an image which is actually present. This probability is given by $(1 - \beta)$ where β is the probability of a correct detection. The probability of a correct detection is the crosshatched area under the $p_1(I)$ curve.

$$\beta = \int_0^{I_T} p_1(I)\, dI \tag{8}$$

The shape of the p.d.f.'s p_0 and p_1 are determined by

- The statistical properties of the speckle;
- The intensity transmittance of $B(x,y)$;
- The intensity transmittance of the ground glass and disk image;

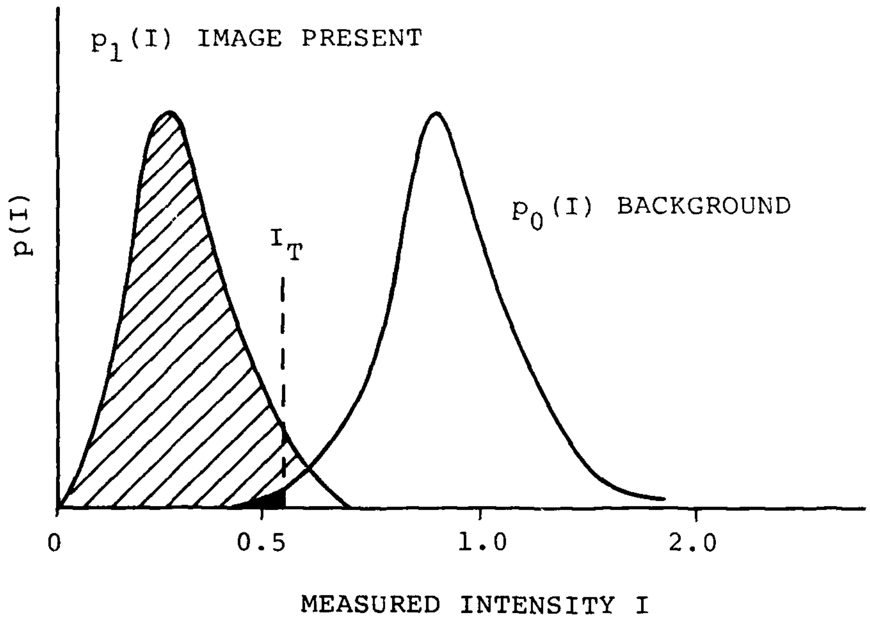

Figure 4. Single threshold detection.

and the distance between the p.d.f.'s is determined by the average value of the intensity transmittance of the disk and ground glass.

VI. PROBABILITY DENSITY FUNCTIONS

An approximate expression for P_0 and P_1 [6] is

$$p(I) \doteq \frac{\left(\frac{M}{\langle I \rangle}\right)^M I^{M-1} \exp\left(-\frac{MI}{\langle I \rangle}\right)}{\Gamma(M)} \tag{9}$$

for $I > 0$, zero otherwise. Where $\Gamma(X)$ is the gamma function, $M = (\langle I \rangle/\sigma_I)^2$, $\langle I \rangle$ average value of the p.d.f. and σ_I is the standard deviation.

VII. CALCULATION OF α AND β

In order to proceed with the calculation of α and β, we need to calculate the mean $\langle I \rangle$ and the standard deviation σ_I of the p.d.f.'s when an image is present and not present.

<u>$p_0(I)$ [No Disk Present]</u>

$$\langle I \rangle_{nd} = I \langle T_S \rangle \tag{10}$$

$$(\sigma_I)^2_{nd} = \langle I \rangle_{nd} \iint_{-\infty}^{\infty} N_{nd}(u, v) \, |b(u, v)|^2 \, dudv \tag{11}$$

where $b(u, v)$ is the Fourier transform of $B(x, y)$.

$$N_{nd}(u, v) = K_{nd} |F(u, v)|^2 * |F(-u, -v)|^2 \tag{12}$$

where $F(u, v)$ is the aperture of the filter in plane P_2. The constant K_{nd} can be evaluated from the fact that

$$\int_{-\infty}^{\infty} p_0(I) \, dI = 1. \tag{13}$$

Once $\langle I \rangle_{nd}$ and $(\sigma_I)_{nd}$ are evaluated, they can be substituted into Equation (9) to obtain $p_0(I)$.

$p_1(I)$ [Disk Present]

$\langle I\rangle_d$ is obtained through the evaluation of Equation (3) using Equations (4) and (5), and $(\sigma_I)_d$ is given by

$$(\sigma_I)_d^2 = \langle I\rangle_d \iint_{-\infty}^{\infty} N_d(u, v) \, |b(u, v)|^2 \, du dv \tag{14}$$

where b(u, v) is again the Fourier transform of B(x, y) and

$$N_d(u, v) = K_d |F(u, v)|^2 * |F(-u, -v)|^2 \tag{15}$$

where F is the same as above. K_d is evaluated as above by noting that

$$\int_{-\infty}^{\infty} p_1(I) \, dI = 1. \tag{16}$$

When the two p.d.f.'s are found, α and β can be calculated

$$\alpha = \int_0^{I_T} p_0(I) \, dI$$

$$\alpha = \int_0^{I_T} \frac{\left(\frac{M}{\langle I\rangle_{nd}}\right)^M I^{M-1} \exp\left(-\frac{MI}{\langle I\rangle_{nd}}\right)}{\Gamma(M)} \, dI \tag{17}$$

where

$$M = \frac{\langle I\rangle_{nd}^2}{(\sigma_I)_{nd}^2}$$

$$\beta = \int_0^{I_T} p_1(I) \, dI$$

$$\beta = \int_0^{I_T} \frac{\left(\frac{M}{\langle I\rangle_d}\right)^M I^{M-1} \exp\left(-\frac{MI}{\langle I\rangle_d}\right)}{\Gamma(M)} \, dI \tag{18}$$

where

$$M = \frac{\langle I \rangle_d^2}{(\sigma_I)_d^2} \, .$$

VIII. CONCLUSIONS

We can note how the size of the disk, the intensity transmissivity and the size of the scanning aperture affect the calculation of α and β.

Parameter	α	β
d size of disk	-	Eq. (3) $\langle I \rangle_d$
T_i disk transmittance	-	Eq. (3) $\langle I \rangle_d$
T_S g.g. transmittance	Eq. (6) $\langle I \rangle_{nd}$	Eq. (3) $\langle I \rangle_d$
D size of aperture	Eq. (6) $\langle I \rangle_{nd}$	Eq. (3) $\langle I \rangle_d$
in plane P_2	Eq. (11) $(\sigma_I)_{nd}$	Eq. (14) $(\sigma_I)_d$
dP size of scanning	Eq. (1) $\langle I \rangle_{nd}$	Eq. (1) $\langle I \rangle_d$
aperture	Eq. (11) $(\sigma_I)_{nd}$	Eq. (14) $(\sigma_I)_d$

REFERENCES

1. See, for example, the special issue of Journal of the Optical Society of America, J. Opt. Soc. Am., 66 (1976).

2. J. C. Dainty, Optica Acta, 18, 327 (1971).

3. B. D. Guenther, N. George, C. R. Christensen and J. S. Bennett, Phot. Sci. Eng., 21, 192 (1977).

4. N. George, C. R. Christensen, J. S. Bennett and B. D. Guenther, J. Opt. Soc. Am., 66, 1282 (1976).

5. C. W. Helstrom, Statistical Theory of Signal Detection, Pergamon Press, London, 2nd ed., 1968, p. 76.

6. J. W. Goodman, "Statistical Properties of Laser Speckle Patterns," in Laser Speckle and Related Phenomena, ed. J. C. Dainty, Springer Verlag, Berlin, 1975, p. 53.

DISTRIBUTION

	No. of Copies
Commander Defense Documentation Center ATTN: DDC-TCA Cameron Station Alexandria, Virginia 22314	12
Commander US Army Research Office ATTN: Dr. R. Lontz P.O. Box 12211 Research Triangle Park, North Carolina 27709	2
US Army Research and Standardization Group (Europe) ATTN: DRXSN-E-RX, Dr. Alfred K. Nedoluha Box 65 FPO, New York 09510	2
US Army Material Development and Readiness Command ATTN: Dr. Gordon Bushy Dr. James Bender Dr. Edward Sedlak 5001 Eisenhower Avenue Alexandria, Virginia 22333	1 1 1
Headquarters Hq DA (DAMA-ARZ) Washington, DC 20301	2
Director of Defense Research and Engineering Engineering Technology ATTN: Mr. L. Weisberg Washington, DC 20301	2
Director Defense Advanced Research Project Agency/STO ATTN: Commander T.F. Wiener D.W. Walsh 1400 Wilson Boulevard Arlington, Virginia 22209	1 1

DISTRIBUTION (Continued)

	No. of Copies
Commander US Army Aviation Systems Command 12th and Spruce Streets St. Louis, Missouri 63166	1
Director US Army Air Mobility Research and Development Laboratory Ames Research Center Moffett Field, California 94035	1
Commander US Army Electronics Research and Development Command ATTN: DRSEL-TL-T, Dr. Jacobs DRSEL-CT, Dr. R. Buser DELEW-E, Henry E. Sonntag Fort Monmouth, New Jersey 07703	 1 1 1
Director US Army Night Vision Laboratory ATTN: John Johnson Mr. John Deline Mr. Peter VanAtta Fort Belvoir, Virginia 22060	 1 1 1
Commander US Army Picatinny Arsenal Dover, New Jersey 07801	1
Commander US Army Harry Diamond Laboratories 2800 Powder Mill Road Adelphi, Maryland 20783	1
Commander US Army Foreign Science and Technology Center ATTN: W.S. Alcott Federal Office Building 220 7th Street, NE Charlottesville, Virginia 22901	1
Commander US Army Training and Doctrine Command Fort Monroe, Virginia 22351	1

DISTRIBUTION (Continued)

	No. of Copies
Director Ballistic Missile Defense Advanced Technology Center ATTN: ATC-D	1
ATC-O	1
ATC-R	1
ATC-T P.O. Box 1500 Huntsville, Alabama 35808	1
Commander US Naval Air Systems Command Missile Guidance and Control Branch Washington, DC 20360	1
Chief of Naval Research Department of the Navy Washington, DC	1
Commander US Naval Air Development Center Warminster, Pennsylvania 18974	1
Commander US Naval Ocean Systems Center Code 6003 Dr. Harper Whitehouse San Diego, California 92152	1
Director Naval Research Laboratory ATTN: Dave Ringwolt	1
Code 5570, T. Gialborinzi Washington, DC 20390	1
Commander Rome Air Development Center US Air Force ATTN: James Wasielewski, IRRC Griffiss Air Force Base, New York 13440	1
Commander US Air Force, AFOSR/NE ATTN: Dr. J.A. Neff Building 410 Bolling Air Force Base Washington, DC 20332	1

DISTRIBUTION (Continued)

	No. of Copies
Commander	
US Air Force Avionics Laboratory	
ATTN: D. Rees	1
W. Schoonover	1
Dr. E. Champaign	1
Dr. J. Ryles	1
Gale Urban	1
David L. Flannery	1
Wright Patterson Air Force Base, Ohio 45433	
Commander	
AFATL/LMT, Charles Warren	1
Eglin Air Force Base, Florida 32544	
Environmental Research Institute of Michigan	
Radar and Optics Division	
ATTN: Dr. A. Kozma	50
Dr. C. C. Aleksoff	1
Juris Upatnieks	1
P.O. Box 618	
Ann Arbor, Michigan 41807	
IIT Research Institute	
ATTN: GACIAC	1
10 West 35th Street	
Chicago, Illinois 60616	
Dr. J. G. Castle	
Physics Department	
University of Alabama	
4701 University Drive, N.W.	
Huntsville, Alabama 35807	1
Science and Technology Division	
Institute of Defense Analysis	
ATTN: Dr. Vincent J. Corcoran	1
400 Army-Navy Drive	
Arlington, Virginia 22202	
Optical Science Consultants	
ATTN: Dr. D.L. Fried	1
P.O. Box 388	
Yorba Linda, California 92686	

DISTRIBUTION (Continued)

	No. of Copies
Commander Center for Naval Analyses ATTN: Document Control 1401 Wilson Boulevard Arlington, Virginia 22209	1
Raytheon Company ATTN: A.V. Jelalian 528 Boston Post Road Sudbury, Massachusetts 01776	1
Dr. J. W. Goodman Information Systems Laboratory Department of Electrical Engineering Stanford University Stanford, California 94305	1
Eric G. Johnson, Jr. National Bureau of Standards 325 S. Broadway Boulder, Colorado 80302	
M. Vanderlind Battelle Columbus Labs 505 Ring Ave. Columbus, Ohio 43201	1
Dr. Nicholas George The Institute of Optics University of Rochester Rochester, New York 14627	1
Naval Avionics Facility Indianapolis, Indiana 46218	1
F. B. Rotz Harris Corporation P.O. Box 37 Melbourne, Florida 32901	1
Robert L. Kurtz TAI Corporation 8302 Whitesburg Dr., S.E. Huntsville, Alabama 35802	1

DISTRIBUTION (Continued)

	No. of Copies
J.R. Vyce Itek Corporation 10 Maguire Road Lexington, Massachusetts 02173	1
Dr. David Cassasent Carnegie Mellon University Hamerschage Hall, Room 106 Pittsburgh, Pennsylvania 15213	1
David M. Karnes McDonnell Douglas Astronautics 5301 Boisa Ave. Huntington Beach, California 92647	1
Professor Anil K. Jain Department of Electrical Engineers University of California, Davis Davis, California 95616	1
Gerald B. Brandt Westinghouse Electric Corporation Research and Development Center Pittsburgh, Pennsylvania 15235	1
K.G. Leib Research Department Grumman Aerospace Corporation Bethpage, New York 11714	1
Terry Turpin Department of Defense 9800 Savage Road Fort George G. Meade, Maryland 20755	1
Dr. Stuart A. Collins Electrical Engineering Department Ohio State University 1320 Kennear Road Columbus, Ohio 43212	1
Mike Scarborough, MS-19 Teledyne Brown Engineering Cummings Research Park Huntsville, Alabama 35807	1

DISTRIBUTION (Continued)

	No. of Copies
Commander AFEL Hanscom Air Force Base, Maryland 01731	1
Dr. Arthur N. Chester	1
Dr. Donald H. Close	1
Thomas R. O'Meara	1
Dr. Wilfried O. Eckhardt Hughes Research Laboratories 3011 Malibu Canyon Road Malibu, California 90265	1
H.J. Caulfield Aerodyne Research, Inc. Bedford Research Park Crosby Drive Bedford, Massachusetts 01730	1
TRW Defense and Space Systems Group One Space Park ATTN: Dr. Peter O. Clark Redondo Beach, California 90278	1
US Army Materiel Systems Analysis Activity ATTN: DRXSY-MP Aberdeen Proving Ground, Maryland 21005	1
DRCPM-PE-E, John Pettitt	1
DRSMI-LP, Mr. Voigt	1
DRSMI-R, Dr. Kobler	1
DRCPM-PE	1
DRSMI-RN, Jerry Hagood	1
-RE, W. Pittman	1
Lewis G. Minor	1
-RD	3
-RG	1
-RG, James A. McLean	1
-O	1
-Y	1

DISTRIBUTION (Concluded)

		No. of Copies
DRSMI-RR,	Dr. R. L. Hartman	1
	Dr. J. S. Bennett	1
	Dr. C. R. Christensen	100
	Dr. J. D. Stettler	1
-RPT	(Reference Copy)	1
-RPT	(Record Set)	1
-RPR		1
		3

LMED

-8